Colloid Polym Sci 279:214–220 (2001)

ORIGINAL CONTRIBUTION

K. Gotoh
M. Tagawa
N. Ohmae
H. Kinoshita
M. Tagawa

Surface characterization of atomic oxygen beam-exposed polyimide films using contact angle measurements

Received: 4 December 1999
Accepted: 31 August 2000

K. Gotoh (✉)
Faculty of Education
Kyoto University of Education
1 Fukakusa-fujinomori-cho
Fushimi-ku, Kyoto 612-8522, Japan
e-mail: keiko@kyokyo-u.ac.jp
Fax: +81-75 645 1734

M. Tagawa · N. Ohmae
Department of Mechanical Engineering
Kobe University, 1-1 Rokko-dai, Nada
Kobe, Hyogo 657-8501, Japan

H. Kinoshita
Department of Material and Life Science
Osaka University, 2-1 Yamada-oka, Suita
Osaka 565-0871, Japan

M. Tagawa
Division of Environmental Engineering
Kanazawa Institute of Technology
7-1 Ohgigaoka, Nonoichi
Ishikawa 921-8501, Japan

Abstract Polyimide surfaces exposed to simulated low Earth orbit space environment, i.e., under hyperthermal atomic oxygen bombardment, were characterized by using atomic force microscopy, X-ray photoelectron spectroscopy, and contact angle measurements. The surface analytical results showed that the roughness and the O/C ratio at the atomic oxygen-exposed polyimide surface increased with increasing atomic oxygen fluence. The advancing and receding contact angles decreased with increasing O/C ratios at the polyimide surfaces. The Lifshitz-van der Waals component, the acid and base parameters of the surface free energy of polyimide films were calculated from the contact angles. The base parameter increased with increasing O/C ratio, whereas the acid parameter and the Lifshitz-van der Waals component did not show a remarkable change. These analytical results agree with the *in situ* XPS data showing the formation of surface functional groups due to atomic oxygen exposure. It was demonstrated in this study that the polyimide surface in a low Earth orbit space environment may become hydrophilic due to the bombardment by atomic oxygen.

Key words Polyimide · Atomic oxygen · Atomic force microscopy · X-ray photoelectron spectroscopy · Contact angle · Surface free energy

Introduction

The oxidation of polymeric materials in a low Earth orbit (LEO), which is 200–700 km above sea level, is one of the major concerns in the field of spacecraft engineering over the last decade. Oxidation of polymers in LEO is due to the collision with ground-state atomic oxygen (AO) which is the dominant (>95%) species of the upper atmosphere of the Earth [1]. The flux and collisional energy of AO with spacecraft surfaces are as high as 10^{19} atoms/m^2/s and 5 eV because of the high orbital velocity of spacecraft (8 km/s). Such a high-energy collision with chemically active AO leads to the material degradation of the exterior surfaces of spacecraft. Since polyimide (PI) has widely been used as a passive thermal control material to cover exterior surfaces of satellites or space structures, PI is one of the key materials to be investigated in AO reactivity. Some experimental studies have already been carried out both on the ground and in in-flight experiments [2–4]. However, most of the ground-based research has ignored the collisional energy factor due to the difficulty in forming a 5 eV AO beam in ground-based facilities. Thus, basic knowledge of the interaction between energetic AO and polymer surfaces has not been studied extensively using the ground-based experiments. On the other hand, the in-flight experiments have been disturbed by severe contamination during the space flight. Once the PI surface is contaminated during the flight, the AO reaction with PI is difficult to analyze after

retrieval. Moreover, the attachment of contamination affects the surface properties of PI films and influences the function of the thermal control system of spacecraft. Due to the requirements for longer operation of spacecraft, avoidance and elimination of the contamination at PI surfaces become more and more important. In general, the surface free energy of solids is one of the major factors governing the contamination attachment. Since the PI surface is considered to be contaminated after AO exposure in LEO, the evaluation of the surface free energy of PI in a simulated LEO space environment is valuable for predicting the contamination behavior of PI surfaces in the LEO space environment.

On the other hand, the use of the 5 eV AO beam formed by the recently developed laser-detonation source is advantageous also for basic polymer studies as well as space applications. Unlike other plasma modification techniques, the laser-detonation source generates high purity, ground state atom/molecular beam with translational energies being tunable from 1–20 eV. In such a translational energy range, physical sputtering is negligible and surface chemical reactions play the major role in surface modification. A recent study using this type of beam source clarifies the presence of the collision-induced beam-surface interactions with PI surfaces [5]. Since the significant role of the adsorbed oxygen is mentioned in the gasification reaction of PI [6], this new chemical reaction scheme may be accompanied with the adsorbed oxygen which may lead to a change of the surface free energy as well. A study of surface free energy at the AO-exposed PI surfaces provides information for a better understanding of the interaction between energetic AO and PI surfaces as well as for establishing a method for contamination control at PI surfaces in LEO space environments.

In the present study, we investigated the surface free energy of AO-exposed PI surfaces. The laser-detonation AO source developed for simulating the LEO space environment was used for this purpose. The surface free energies of pristine and AO-exposed PI films were determined by the contact angles measured using the Wilhelmy and the sessile drop methods. Chemical and topological characteristics of the AO-exposed PI surfaces were characterized using X-ray photoelectron spectroscopy (XPS) and atomic force microscopy (AFM). The effect of AO exposure on the contact angle and on surface free energy at PI surfaces are discussed.

Materials and methods

Materials

The PI samples used were pyromelitic dianhydride-4, 4′-oxydianiline (PMDA-ODA) PI, commercially available from DuPont (Kapton-H). The thickness of the PI film was 25 μm. Prior to use, the PI films were purified with water, ethanol, and diethyl ether by applying ultrasonic waves. Water was deionized and doubly distilled using a borosilicate glass apparatus.

Atomic oxygen exposure

The AO beam facility used in this study was based on the laser-detonation phenomenon [5]. Details of the facility are described elsewhere [7, 8]. The CO_2 laser light was focused on the nozzle throat at the moment when a pulsed supersonic valve introduced pure oxygen gas into the nozzle. The AO beam was characterized by a time-of-flight (TOF) distribution measured by a quadrupole mass spectrometer as a detector. From a TOF distribution, the mean energy of the hyperthermal AO beam was calculated to be 4.5 eV. The AO flux of the beam was measured by an Ag-coated quartz crystal microbalance [9] and was typically 3×10^{17} atoms/m^2/s at the sample position.

The PI surfaces before and after AO beam exposures were characterized by XPS consisting of a double-pass cylindrical mirror analyzer (DESA-100, Staib Instrumente GmbH, Germany) and a non-monochromatic dual anode X-ray source (TA-10, VSW, England). The surface roughness of the samples was analyzed by AFM (Nanoscope IIIa, Digital Instruments, USA).

Contact angle measurements

In the present study, the contact angle measurement was carried out both by the Wilhelmy method and by the sessile drop method to measure the advancing and receding contact angles of the film with the different wettability at each side of the film. In the Wilhelmy method, an electrobalance (Model C-2000, Cahn Instruments Inc., USA) and a reversible elevator (Inchworm Motor Model 6000, Burleigh Instruments Inc., USA) were utilized to measure the contact angle [10–15]. A PI film (0.3–0.6 mm in width and 4–5 mm in length) was suspended from the arm of an electrobalance. A beaker containing a probe liquid was raised by an elevator so that the liquid surface reached 2–3 mm higher than the lower edge of the film (immersion). Then the beaker was moved down to the original position (emersion). A continuous weight recording was made during an immersion-emersion cycle at an interfacial moving rate of 0.3 mm/min [11, 12]. The immersion-emersion cycle was repeated twice and the reproducibility of the weight recording was confirmed. The contact angle was calculated from the wetting force using the Wilhelmy equation [11]. The effective perimeter of the film was calculated from the wetting force at the pentane/air interface because the contact angle in this system can be assumed to be zero [11].

The sessile drop experiments were performed using a video contact angle system (VCA-2500, ASC products, USA). A liquid drop of 2–3 μL was placed at the film surface using a microsyringe [16, 17]. The drop was viewed using a CCD camera attached to a microscope. The drop image was digitized and stored in a computer every second during the measurement. The contact angle and the drop base diameter of each frame were measured by placing markers on the circumference of the drop image on a monitor.

Determination of surface free energies of PI films

The Young-Good-Girifalco-Fowkes equation including acid-base interaction terms can be written as [18]:

$$\gamma_L(1+\cos\theta) = 2\left(\sqrt{\gamma_s^{LW}\gamma_L^{LW}} + \sqrt{\gamma_s^{+}\gamma_L^{-}} + \sqrt{\gamma_s^{-}\gamma_L^{+}}\right) \quad (1)$$

where θ is the contact angle of the liquid, γ is the surface free energy; the subscripts S and L refer to solids and liquids, respectively, and the superscripts LW, +, and − refer to the Lifshitz-van der Waals component, the Lewis acid parameter, and

the Lewis base parameter, respectively. In order to solve the three unknowns for solids, i.e., γ_S^{LW}, γ_S^+ and γ_S^-, it is necessary to determine the contact angles with three completely characterized liquids [19]. Therefore, the advancing contact angles of three pure liquids (water, diiodomethane, and ethylene glycol) on the PI films were measured by the sessile drop method. The surface free energies of solids, i.e., γ_S^{LW}, γ_S^+ and γ_S^- were calculated using Eq. 1 with the contact angles, θ, and the published values of γ_L^{LW}, γ_L^+ and γ_L^- [19].

Results and discussion

XPS analysis

Figure 1 shows the high-resolution XPS spectra of the pristine and AO-exposed (AO fluence of 5.9×10^{21} atoms/m^2) PI surfaces. The XPS measurement was made with 200 W Mg-Kα X-rays with an average take-off angle of 45° in UHV conditions. The deconvolution procedure of the XPS spectra is described elsewhere [3] but is briefly explained here. On the basis of the molecular orbital calculation of PI reported by Silverman et al. [20] and of the experimental database reported by Beamson and Briggs [21], the carbon atoms in the PI structure were categorized in 4 groups for the pristine sample and in 6 groups for the AO-exposed samples. The major peaks of the 4 groups were 285.0, 286.0, 286.6, and 288.9 eV for the C1s spectrum for the pristine PI: the first, 285 eV, is attributed to eight carbon atoms in ODA; the second, 286 eV, is due to six carbon atoms in PMDA and carbon singly bonded to nitrogen; the third, 286.6 eV, is due to two carbon atoms singly bonded to oxygen in the ODA; and, finally, 288.9 eV is due to the carbonyl group in the PMDA chain [6]. Two peaks were added for the deconvolution of the AO-exposed PI, being 287.7 and 289.6 eV, which correspond to carbonyl and carboxyl groups, respectively. The compensation of the surface charging effect was made by using the N1s peak position as a reference. The results of compensation was also verified by the peak position of carboxyl carbon in the C1s spectrum. The shake-up satellites in the C1s and O1s were not considered in the peak fitting results because of the insufficient signal to noise ratio of the spectra. Comparing the C1s XPS spectra of AO-exposed PI films with pristine ones, it was found that AO exposure leads to an increase of oxidized states of carbon atoms in the PI structure (carbonyl and carboxyl). The change in the C1s XPS peak due to AO exposure is fairly large compared with those reported previously [3]. This is due to the large AO fluence and the effect of not suffering air exposure before the XPS measurements [6]. As for the O1s spectra, there exist two peaks with the original surface. The peak of 532.0 eV is due to the imide carbonyl groups, while the peak of 533.3 eV is due to the ether-type oxygen species. Two additional peaks were added to synthesize the O1s spectrum of the AO-exposed polyimide, being 531.3 and 533.9 eV, which are possibly due to -CH_2-C(O)-NH- and -(C=O)-O-(C=O)- structures [21]. The N1s peak centered at 400.6 eV is assigned to imide nitrogen species. No significant change in the N1s spectrum was observed after exposure. The change in XPS spectra suggests the scission of the C—N bond in PMDA and the formation of functional groups such as carbonyl and carboxyl groups at this location. These

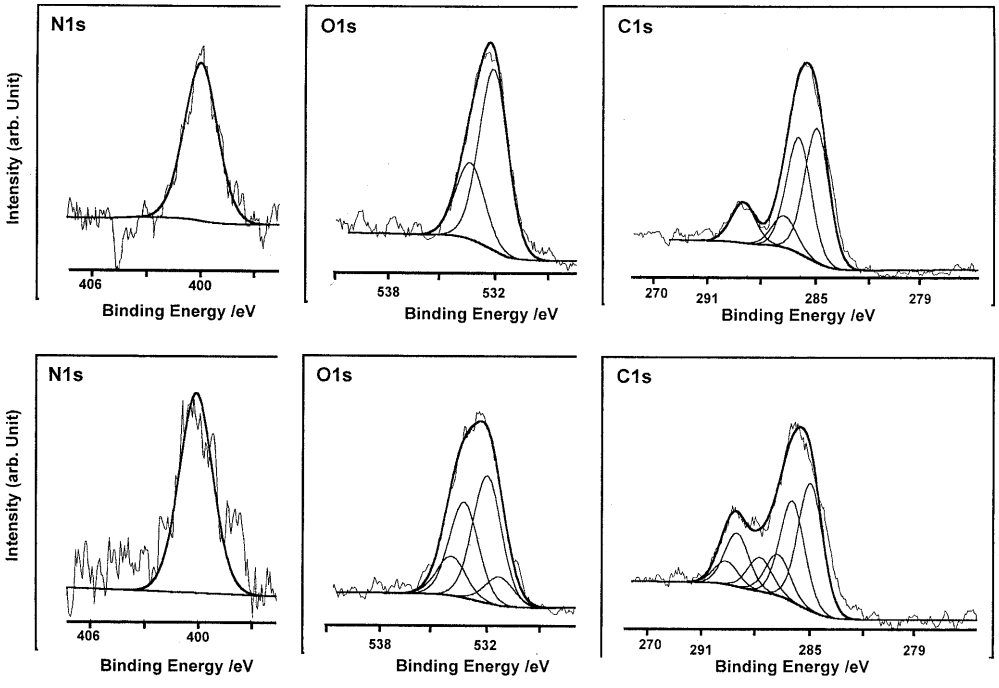

Fig. 1 The XPS core level spectra of N1s, O1s and C1s of the pristine PI film (upper panels) and the AO-exposed PI film at AO fluence of 5.9×10^{21} atoms/m^2 (lower panels)

analytical results are consistent with the conclusion obtained using the ion beam-type AO source [3].

The peak areas were divided by the atomic sensitivity factors of the respective elements (C1s: 1.00, N1s: 1.77 and O1s: 2.85) to calculate the atomic concentrations of carbon, oxygen and nitrogen. It was found that the oxygen concentration increased with AO exposure, whereas the nitrogen concentration was almost constant at 6–10%. Figure 2 shows the O/C ratio as a function of total AO fluence. One finds that the O/C ratio increased with AO fluence and reached the saturation value of O/C = 0.45 at the AO fluence of 3×10^{21} atoms/m^2. It is concluded that the PI surface becomes a steady-state oxidized surface from the AO beam exposure with an AO fluence of 3×10^{21} atoms/m^2.

Effect of atomic oxygen exposure on contact angles and surface free energies

The weight recording measured by the Wilhelmy method in the pristine PI/water/air system is presented in Fig. 3. The points "a", "b", and "c" show the moments when the lower edge of the PI film touched the water surface, when the direction of the motion of the water surface was reversed, and when the lower edge of the film was separated from the water surface, respectively. It is obvious that the weights during the advancing and receding scans were almost constant, although the local deviation of the wetting force was obvious. This is due to a deviation in the local contact angle and/or perimeter of the film along with the line of contact. The advancing and receding contact angles were calculated from the changes in weight at the points "a" and "c", which correspond to the advancing and receding wetting forces, W_a and W_r, respectively.

Figure 4 shows the contact angle data for the pristine PI film measured by the sessile drop method. The contact angles of water on the film are plotted as a function of time. The contact angle linearly decreased with time at the initial stage of the measurement (see the inset in Fig. 4). At this stage, the drop base diameter increased and, hence, the water front advanced. Therefore, the contact angle extrapolated to time-zero was determined as an advancing contact angle. After a certain period, the contact angle decreased and became almost constant. In this stage, the drop base diameter decreased due to the vaporization of the liquid, i.e., the water front receded. Therefore, the contact angle showing the constant value was treated as the receding contact angle. The determination of the advancing and receding contact angles using the sessile drop technique has been made by adding or withdrawing a small volume

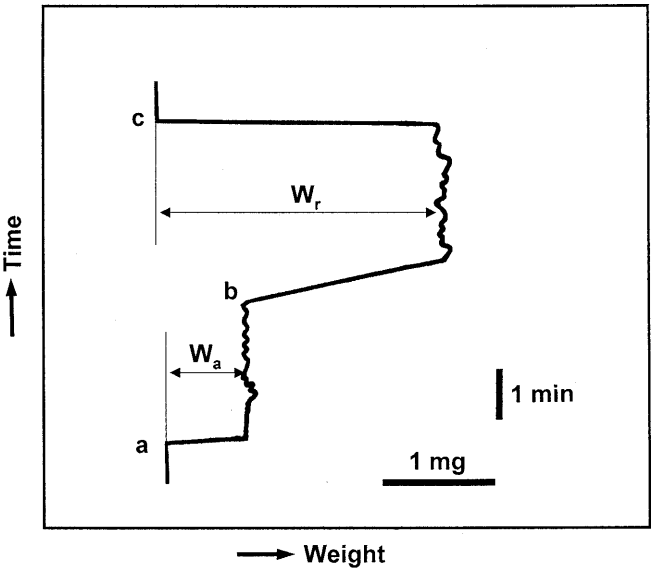

Fig. 3 The weight recording for the pristine PI film at the water/air interface

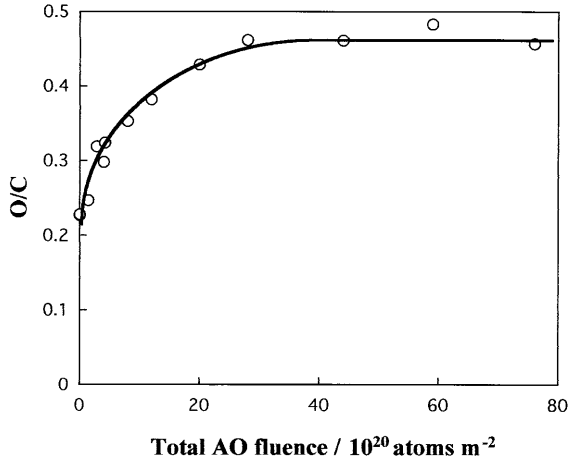

Fig. 2 The O/C ratio at the PI surface as a function of total AO fluence

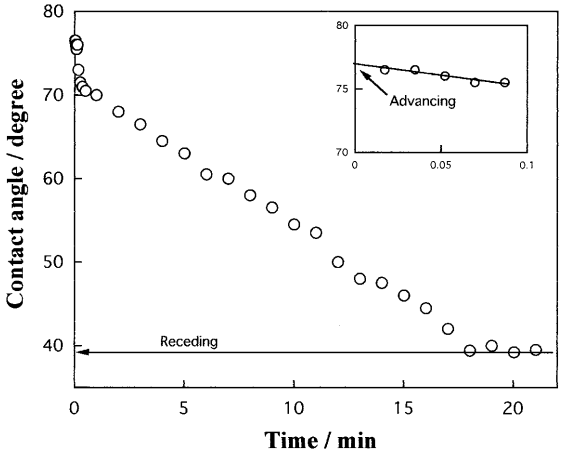

Fig. 4 Change in the contact angle of water on the pristine PI film as a function of time

of the liquid [22]. The contact angles, thus measured, are often interpreted in terms of advanced and receded angles [23]. In the present study, we propose a new method for evaluating the advancing and receding contact angles by the sessile drop technique. The advancing and receding contact angles measured by the sessile drop method in this study (76.9° and 39.5°) showed good agreement with those measured by the Wilhelmy method (76.4° and 38.2°). The agreement justifies the method for evaluating the advancing and receding angles by the sessile drop technique proposed in this study.

The AO exposure of the PI sample was carried out only on one side of the sample. In the wetting force measurement of the AO-exposed PI samples using the Wilhelmy method, the total wetting force is considered to be the sum of the wetting forces at the AO-exposed side and at the unexposed side of the specimen. Therefore, the contact angle of the AO-exposed surface was calculated by subtracting the wetting force of the unexposed side using the contact angle of the pristine PI. The contact angles of the AO-exposed side, thus calculated, were compared with those measured by the sessile drop method. The Wilhelmy method determined the advancing and receding contact angles of the AO-exposed surface to be 74.4° and 26.3°, whereas using the sessile drop measurement they were 74.0° and 27.6°, respectively. The consistency in the contact angles obtained by the two procedures showed the propriety of the proposed data-processing by the Wilhelmy method.

Figure 5 shows the contact angles of water as a function of AO fluence. With increasing AO fluence, both the advancing and receding contact angles decreased, i.e., the wettability increased. The contact angles were replotted against the O/C ratio measured by XPS. The results are shown in Fig. 6. Both the advancing and the receding contact angles linearly decreased with increasing O/C ratio. The behavior of contact angles as observed in the present study is consistent with the theoretical calculations of the contact angles on the heterogeneous surfaces as reported by Johnson et al.: both advancing and receding contact angles decrease with increasing percentage in the high-energy region of intermediate surfaces such as in PI film surfaces [23]. In the previous study [13], we had investigated the contact angles of water on AO-exposed carbon fibers using the Wilhelmy method. The results on carbon fibers indicated that the receding contact angle decreased with increasing atomic concentration of oxygen, whereas the advancing contact angle remained constant. This behavior of contact angles is also explained by Johnson's theory, i.e., only receding contact angles decrease with an increasing percentage in the high-energy region of hydrophobic surfaces such as graphitized carbon fibers.

Surface roughness is another factor influencing the contact angles. The degrees of surface roughness of the pristine and the AO-exposed PI films were examined by AFM with mean and root mean square roughness, measured over a 1 μm × 1 μm area. The results are shown in Fig. 7 as a function of total AO fluence. The roughness of the PI surface was found to increase with increasing AO fluence. This is considered to be an early stage of the formation of a "shag-carpet-like structure" which is widely known as a surface texture of the PI exposed to LEO space environment [24]. However, the roughness of the AO-exposed PI surface was small, in the order of a few nanometers. Wenzel stated that the observed contact angle on rough surfaces was not identical to the intrinsic contact angle [25, 26]. According to Wenzel's equation, the observed contact angle can

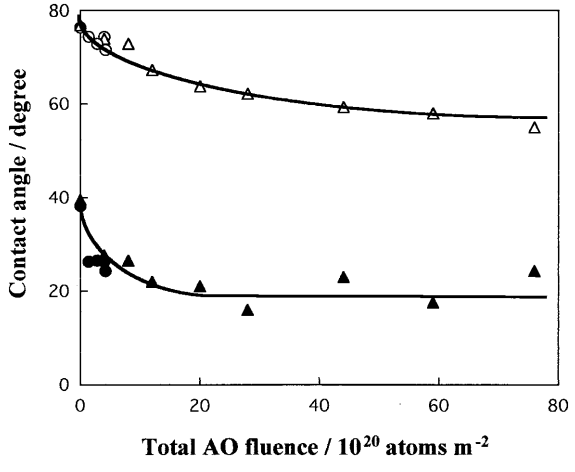

Fig. 5 The advancing (○,△) and receding (●, ▲) contact angles of water on the PI films measured by the Wilhelmy (○, ●) and the sessile drop methods (△, ▲) as a function of total AO fluence

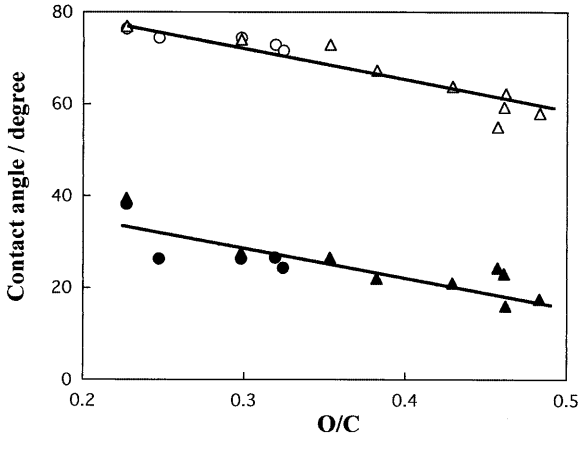

Fig. 6 The advancing (○, △) and receding (●, ▲) contact angles of water on the PI films measured by the Wilhelmy (○, ●) and the sessile drop methods (△, ▲) as a function of O/C ratio at PI surfaces

decrease with increasing surface roughness for contact angles of less than 90°. The contact angles obtained by the Wilhelmy and the sessile drop methods in the present study correspond to the intrinsic and the observed contact angles, respectively. The agreement in the contact angles of the AO-exposed PI measured by the Wilhelmy and the sessile drop methods indicate that the effect of surface roughness in the range of a few nanometers does not affect the contact angle measurements reported in this study.

The Lifshitz-van der Waals component, and Lewis acid and base parameters of the surface free energy of PI films are presented in Fig. 8 as a function of the O/C ratio. The base component increased with increasing O/C ratios whereas the other two components remained constant. This result may be explained by the introduction of surface functional groups due to AO bombardment. The formation of carbonyl and carboxyl groups at the AO-exposed PI surface was clearly detected by XPS as described earlier. These surface functional groups are expected to be electron donors. It is, therefore, concluded that the change in contact angles of PI by the AO beam exposure is due mainly to the increase in the base component of the surface free energy which is explained by the formation of carbonyl and/or carboxyl groups.

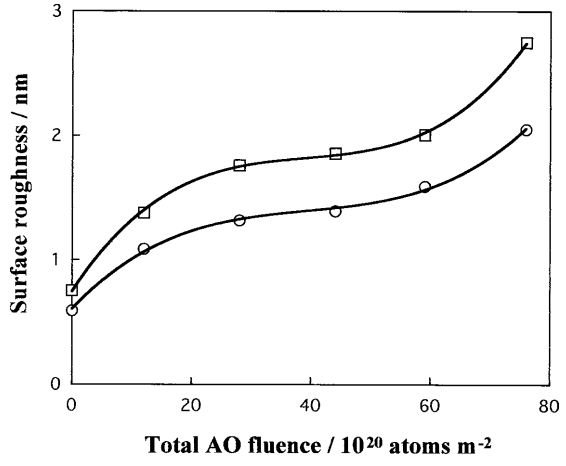

Fig. 7 The mean roughness, R_a, (○) and the root mean square roughness, R_{rms}, (□) at PI film surfaces as a function of total AO fluence

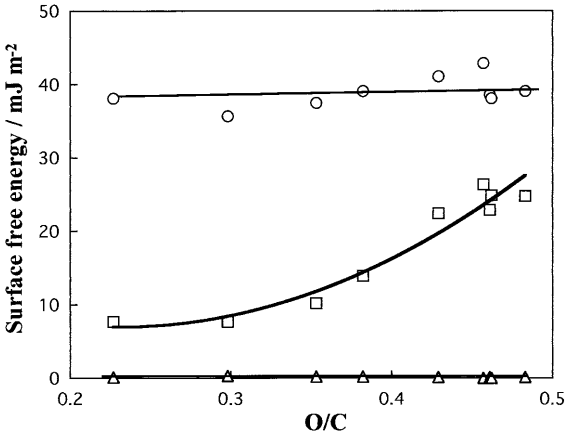

Fig. 8 The Lifshitz-van der Waals component (○), the acid parameter (△), and the base parameter (□) of the surface free energy of PI films as a function of O/C ratio

PI surface in LEO space environment

In this study, XPS measurements were made without ambient air exposure and we observed oxidation of PI surfaces even without air exposure. This result suggests that the surface oxidation can occur in LEO. This conclusion is contradictory to that reported by Grossman et al. [27]: they observed the loss of surface oxygen during AO beam exposure. However, previous research into the effect of air exposure on the AO-exposed PI supports our conclusion which can explain the results of in-flight experiments [6]. The experimental results in this study suggest that the increase in wettability of PI surfaces due to AO bombardment occurs in the LEO space environment. Such a hydrophilic surface easily allows for the attachment of contamination such as dumped water from a spacecraft. Therefore, for the future assessment or modeling of the contamination behavior at PI surfaces in LEO space environment, the influence of the AO-induced hydrophilic effect should be taken into consideration.

Conclusions

The PI surfaces exposed to AO beam with a translational energy of 4.5 eV were characterized by AFM, XPS and contact angle analysis. The AFM and XPS data showed that the roughness and surface oxygen content at the PI surface increased after AO exposure. The contact angles of water on the AO-exposed PI film were found to decrease linearly with increasing O/C ratio at PI surfaces. It was also clear that the decrease in contact angle was due to the increase in the base component of the surface free energy. These experimental results were interpreted to show that the adsorbed oxygen at the AO-exposed PI surface formed surface functional groups which served as electron donors. It was suggested that the increase in wettability of PI surfaces due to AO bombardment occurs in the LEO space environment. Such a hydrophilic PI surface allows for the easy attachment of contamination and may accelerate its performance loss as a thermal control material. Therefore, the AO-induced hydrophilic effect should be considered in a future assessment of material degradation and of contamination attachment in the LEO space environment.

Acknowledgements We would like to thank Miss Y. Suzuki and Miss K. Miyashita of Nara Women's University for their experimental assistance. A part of this work was supported by the Grant-in-Aid for Scientific Research from the Ministry of Education, Science, Sports and Culture, Japan; and by the Space Utilization Promotion Fund from the Japan Space Forum.

References

1. Anderson BJ (ed) (1994) Natural orbital environment guidelines for use in aerospace vehicle development. NASA TM-4527
2. Kleiman JI, Gudimenko YI, Iskanderova ZA, Tennyson RC, Morison WD, McIntyre MS, Davidson R (1995) Surface and Interface Analysis 23:335
3. Kinoshita H, Tagawa M, Umeno M, Ohmae N (1998) Transactions of the Japan Society for Aeronautical and Space Sciences 41:94
4. Brinza DE, Chung SY, Minton TK, Liang RH (1994) Final Report on the NASA/JPL Evaluation of Oxygen Interactions with Materials-3 (EOIM-3). JPL Publication 94–31, California
5. Caledonia GE, Krech RH, Green BD (1987) AIAA Journal 25:59
6. Kinoshita H, Yokota K, Tagawa M, Ohmae N (2000) 8th International Symposium on Materials in a Space Environment, 5th International Conference on Protection of Materials and Structures from the LEO Space Environment. Arcachon, France, in press
7. Kinoshita H, Ninomiya Y, Ikeda J, Tagawa M, Umeno M, Ohmae N (1998) Proc. 21st International Symposium on Space Technology and Science. Omiya, Japan, 98-b-28
8. Tagawa M, Kinoshita H, Ninomiya Y, Kurosumi Y, Ohmae N, Umeno M (1999) Proc. 44th International SAMPE Symposium and Exhibition. Long Beach, USA, p 402
9. Matijasevic V, Garwin EL, Hammond RH (1990) Rev Sci Instrum 61:1747
10. Tagawa M, Ohmae N, Umeno M, Gotoh K, Yasukawa A, Tagawa M (1989) Colloid Polym Sci 267:702
11. Tagawa M, Gotoh K, Yasukawa A, Ikuta M (1990) Colloid Polym Sci 268:589
12. Tagawa M, Ohmae N, Umeno M, Yasukawa A, Gotoh K, Tagawa M (1991) Jpn J Appl Phys 30:2134
13. Tagawa M, Yasukawa A, Gotoh K, Tagawa M, Ohmae N, Umeno M (1992) J Adhesion Sci Technol 6:763
14. Okamura Y, Tagawa M, Gotoh K, Sunaga S, Tagawa T (1996) Colloid Polym Sci 274:628
15. Gotoh K, Yoshimitsu S, Tagawa M (1996) J Adhesion Sci Technol 10:1129
16. Drelich J, Miller JD (1994) J Colloid Interface Sci 164:252–259
17. Drelich J, Wilbur JL, Miller JD, Whitesides GM (1996) Langmuir 1996:1913
18. van Oss CJ, Good RJ, Chaudhury MK (1988) Langmuir 4:884
19. Good RJ (1993) In: Mittal KL (ed), Contact Angle, Wettability and Adhesion. VSP, Utrecht, p 3
20. Silverman BD, Bartha JW, Clabes JG, Ho PS, Rossi AR (1986) J Polym Sci A24:3325
21. Beamson G, Briggs D (1992) High Resolution XPS of Organic Polymers, The Scienta ESCA300 Database, John Wiley & Sons, Chichester
22. Drelich J, Miller JD, Good RJ (1996) J Colloid Interface Sci 179:37
23. Johnson Jr RE, Dettre RH (1993) In: Berg JC (ed), Wettability. Dekker, New York, p 12
24. Whitaker AF, Little SA, Harwell RJ, Griner DB, Detlaya RF, Fromhold Jr. AT (1995) AIAA paper 85–0416
25. Wenzel RN (1936) Ind Eng Chem 28:988
26. Wenzel RN (1949) J Phys Chem 53:1466
27. Grossman E, Lifshitz Y, Wolan JT, Mount CK, Hoflund GB (1999) Journal of Spacecraft and Rockets 36:75